Proceedings of the XVII ECSMGE-2019
Geotechnical Engineering foundation of the future
ISBN 978-9935-9436-1-3

doi: 10.32075/17ECSMGE-2019-1079

XVII European Conference on Soil Mechanics and Geotechnical Engineering
ECSMGE 2019 Reykjavík

Effect of stress on the thermal conductivity of soils

Effet de la contrainte sur la conductivité thermique des sols

H. Hailemariam
Marine and Land Geomechanics and Geotechnics, Kiel University, Kiel, Germany

F. Wuttke
Marine and Land Geomechanics and Geotechnics, Kiel University, Kiel, Germany

ABSTRACT: Effective stress applied over porous media governs the heat transfer behavior and conduction paths of most sensible heat storage and borehole heat exchanger systems, which possess load carrying capacities and are designed as part of the sub-structure of buildings. Nevertheless, the vital role which applied effective stress plays in the heat flow and inter-particle contact condition of porous media has not been given adequate attention, as compared to the other commonly studied governing porous media hydro-mechanical conditions. On this basis, the results of experimental studies of the variations of the thermal conductivities of three silty clay and five sandy soils with effective stress, obtained using a steady state thermal conductivity device are presented in this study. Overall, the findings of the tests, which were conducted in both dry and saturated conditions, show a strong dependence of the thermal conductivity of the soils with effective stress, thus enabling the accurate determination of the thermal conductivity of these porous materials when used in underground heat storage systems, which is a vital parameter in the design and operation of such systems.

RÉSUMÉ: la contrainte effective appliquée sur un milieu poreux régit le comportement du transfert thermique et les chemins de conduction du stockage de la chaleur la plus sensible et des systèmes échangeurs de chaleur de puits de forage, qui possèdent des capacités de support de charge et sont conçus comme une partie de la sous-structure des bâtiments. Cependant, le facteur essentiel, qui a appliqué la contrainte effective, intervient dans le flux thermique, et la condition du contact inter-particulaire des milieux poreux n'a pas été suffisamment prise en compte, par comparaison avec les autres conditions hydromécaniques communément étudiées qui régissent les milieux poreux. A ce titre, les résultats des études expérimentales des variations des conductivités thermiques de trois argiles limoneuses et de cinq sols sablonneux en fonction de la contrainte effective, obtenus en utilisant un dispositif de conductivité thermique à l'état stationnaire, sont présentés dans cette étude. Dans l'ensemble, les conclusions des essais, qui ont été réalisés à la fois dans des conditions sèches et de saturation, révèlent une forte dépendance de la conductivité thermique des sols à la contrainte effective, permettant ainsi la détermination précise de la conductivité thermique de ces matériaux poreux quand ils sont utilisés dans les systèmes souterrains d'accumulation de la chaleur, ce qui constitue un paramètre essentiel dans la conception et l'exploitation de tels systèmes.

Keywords: Thermal conductivity; effective stress; porous media, water content

1 INTRODUCTION

Thermal conductivity plays a vital role in the conductive heat transfer analysis of several engineering applications, such as the operation of small and large scale seasonal thermal energy storages, embedding of underground power cables in porous media, nuclear waste disposal facilities, heat exchanger piles of structures, assessing the effect of berms on the heat loss from thermal energy storage tanks etc. (Hart and Whiddon, 1984; Rosen and Hooper, 1989). One of the fastest growing technologies of seasonal thermal energy storage systems is via sensible heat storage and borehole heat exchanger systems, where heat or cold from solar collectors or other sources of energy is stored for periods of up to several months, for future household and industrial uses. Such systems generally have load bearing capabilites and are typically designed as part of the sub-structure of buildings (Hailemariam and Wuttke, 2018), and hence accurate determination of the thermal conductivity of the sensible heat storage medium and its variations with effective stress must be carefully studied.

On this regard, the variations of the thermal conductivities of three fine-grained and five coarse-grained soils with effective stress, are experimentally studied in this research using a steady state thermal conductivity device.

2 EXPERIMENTAL PROGRAM

2.1 Tested soils

Three silty clay soils (Figure 1), referred here as silty clays A to C (SC-A to SC-C, respectively), and five sandy soils (Figure 2), sands A to E (S-A to S-E, respectively), were investigated. The common geotechnical properties of the soils, obtained following ASTM D 420 - D 5876 (2011), are listed in Tables 1 and 2.

Figure 1. (from left to right) Silty clay soils A to C

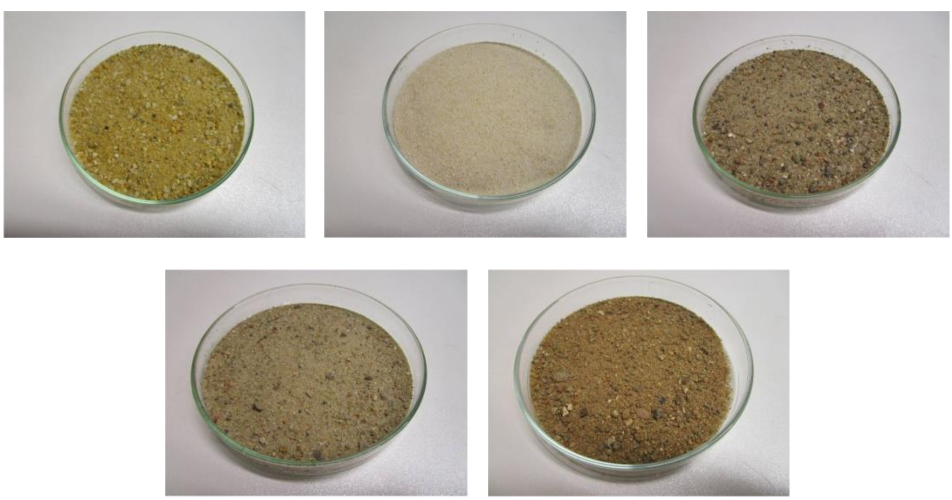

Figure 2. (from left to right) Sandy soils A to E

Table 1. Geotechnical properties of the investigated silty clay soils

Property	**SC-A**	**SC-B**	**SC-C**
Depth (m)	0.3 - 0.7	0.3 - 0.7	0.3 - 0.7
Gravel, > 2 mm (wt.%)	16.1	14.9	2.8
Sand, 0.063 - 2 mm (wt.%)	8.8	12.2	7.1
Silt, 0.002 - 0.063 mm (wt.%)	58.2	52.5	65.4
Clay, < 0.002 mm (wt.%)	16.8	20.2	24.6
Porosity n (-)	0.443	0.464	0.473
Solids specific gravity G_s (-)	2.673	2.670	2.621
Bulk dry density ρ_d (kg m^{-3})	1489	1431	1381
Liquid limit L_L (%)	34.6	43.1	48.2
Plasticity index P_I (%)	14.81	19.45	23.19
Natural gravimetric water content w_n (-)	0.168	0.191	0.194
Unified soil classification system (USCS)	CL	CL	CL

Table 2. Geotechnical properties of the investigated sandy soils

Property	**S-A**	**S-B**	**S-C**	**S-D**	**S-E**
Gravel, > 2 mm (wt.%)	9.62	0	4.78	5.69	9.54
Sand, 0.063 - 2 mm (wt.%)	90.27	100	95.16	94.14	89.95
Silt, 0.002 - 0.063 mm (wt.%)	0.11	0	0.06	0.17	0.51
Clay, < 0.002 mm (wt.%)	0	0	0	0	0
Porosity n (-)	0.347	0.426	0.335	0.335	0.336
Solids specific gravity G_s (-)	2.65	2.65	2.66	2.66	2.65
Bulk dry density ρ_d (kg m^{-3})	1730	1521	1769	1769	1760
Grain diameter at 10% passing D_{10} (mm)	0.27	0.21	0.27	0.21	0.22
Grain diameter at 50% passing D_{50} (mm)	0.64	0.36	0.60	0.40	0.50
Coefficient of uniformity C_u (-)	3.00	1.81	2.63	2.19	2.72
Coefficient of curvature C_c (-)	0.77	1.05	0.88	0.99	0.83
Unified soil classification system (USCS)	SP	SP	SP	SP	SP

2.2 Determination of steady state thermal conductivity

A steady state thermal conductivity and diffusivity meter which works on the principle of the divided bar apparatus technique (Birch and Clark, 1940; McGuinness et al., 2014) is used for analyzing the variation of the effective thermal conductivity of the soils with effective (Figures 3 and 4).

In the divided bar apparatus, the temperature drop across the specimen is compared with that across a disk of standard material of known thermal conductivity. The method is deemed to be the most accurate method of measuring the thermal conductivity of materials in the laboratory with an estimated measurement accuracy of 5% and repeatability variance between 2 and 5% (McGuinness et al., 2014).

The steady state thermal conductivity apparatus consists of a top heating plate, a bottom cooling plate and a PPS Laticonther thermoplastic reference disc with known thermal conductivity (Figure 4). The temperature of the top heating T_1 and bottom cooling T_3 plates is controlled via a circulating fluid (distilled water + glycol), which is pumped using Huber Ministat 125 Pilot ONE heat pumps, and the resulting temperature of the reference plate T_2 is recorded. The specimen is sandwiched between the top heating and reference plates and is laterally insulated by a PMMA Plexiglas sample holder with a very low thermal conductivity. The top and bottom heating/cooling plates consist of extremely thin PT 100 temperature sensors with an accuracy of 0.05°C. The system measures sample deformation or expansion with a TRS-0050 linear transducer with an independent linearity of 0.15% and repeatability of 2μm. Vertical stress (with a maximum force limit of 60 kN) is applied to the specimen via a UL-60 loading machine integrated with the system (Figure 3).

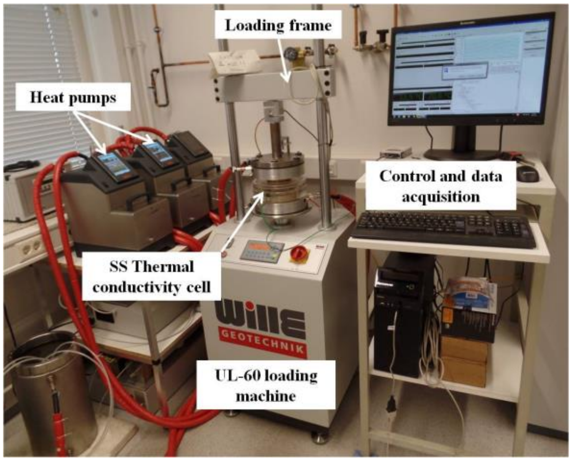

Figure 3. Steady state thermal conductivity measurement setup

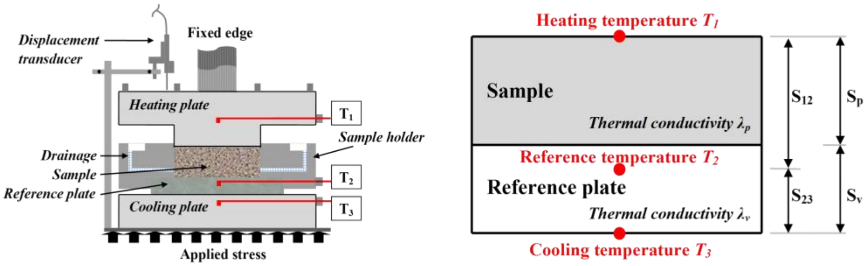

Figure 4. Schematic representation (left) and dimensional analysis (right) of the thermal conductivity cell

The details of the mathematical description of the one dimensional conductive heat transport within the device are provided in Hailemariam and Wuttke (2018). The effective thermal conductivity of the specimen is given by:

$$\lambda_p = \frac{\lambda_v S_p}{\left[\frac{T_1 - T_3}{T_2 - T_3}\right] S_{23} - S_v} \qquad (1)$$

where, T_1, T_2 and T_3 (°C) are the temperatures of the top (heating) plate, reference disc and bottom (cooling) plate, respectively, λ_p and λ_v (W m^{-1} K^{-1}) are the thermal conductivities of the specimen and the reference disc, respectively, S_p, S_v and S_{23} (m) are the distances as shown in Figure 4 (right).

2.3 *Experimental procedure*

The measurements of thermal conductivity of the soils were performed at both dry and saturated conditions using the steady state device (section 2.2). The samples, with dimensions of 100 mm diameter and heights of around 30 mm (except for the saturated silty clays, where the height was 34 mm), were placed carefully in to the thermal cell at the desired saturation condition and by making sure that the bulk density was homogeneous throughout the specimen volume. The temperatures of the top heating and bottom cooling plates were set to the desired values, and once steady state conditions were achieved for each specimen, the effective stress was increased up to 800 kPa at constant rates of 2 and 4 kPa/min for the silty clays soils and sandy soils, respectively. The temperature of the reference plate and deformation of the specimen were simultaneously recorded at an interval of 5 seconds throughout the duration of the tests. The recorded temperatures of the reference plate were used to obtain the steady state thermal conductivity of the samples using Equation 1.

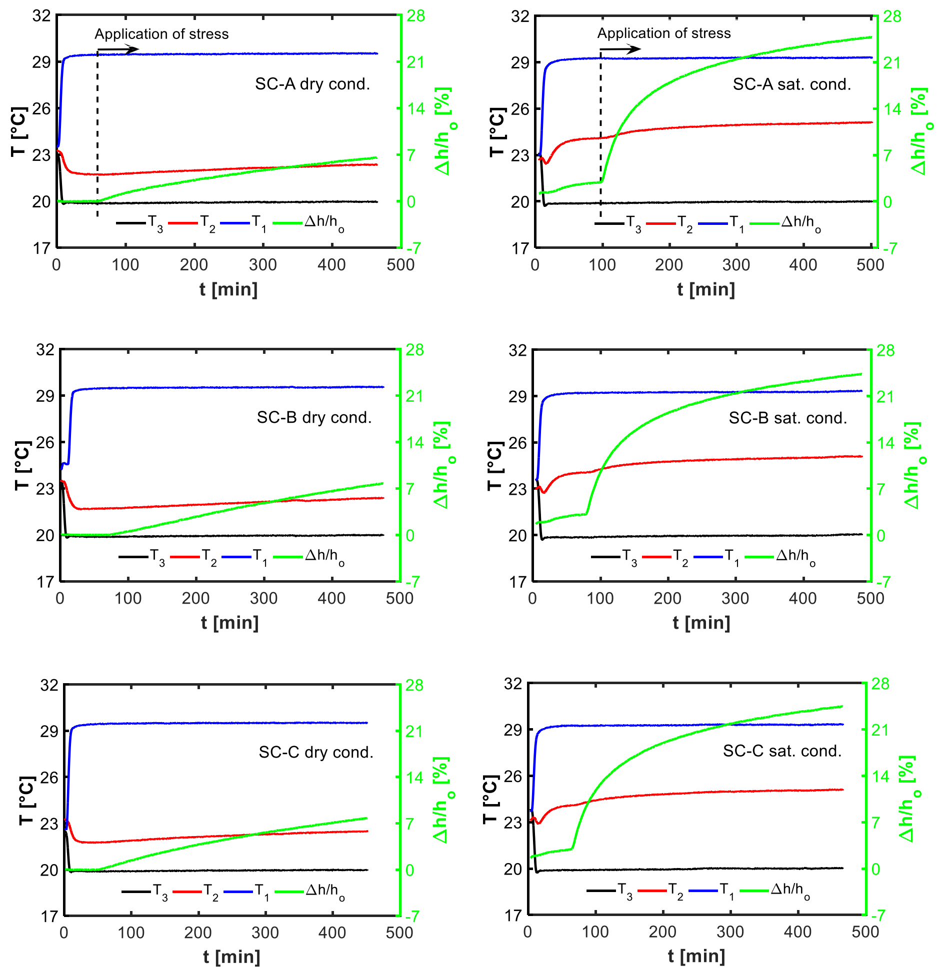

Figure 5. Temperature T and vertical strain $\Delta h/h_o$ plots for the steady state thermal conduction tests of the silty clay soils as functions of time t

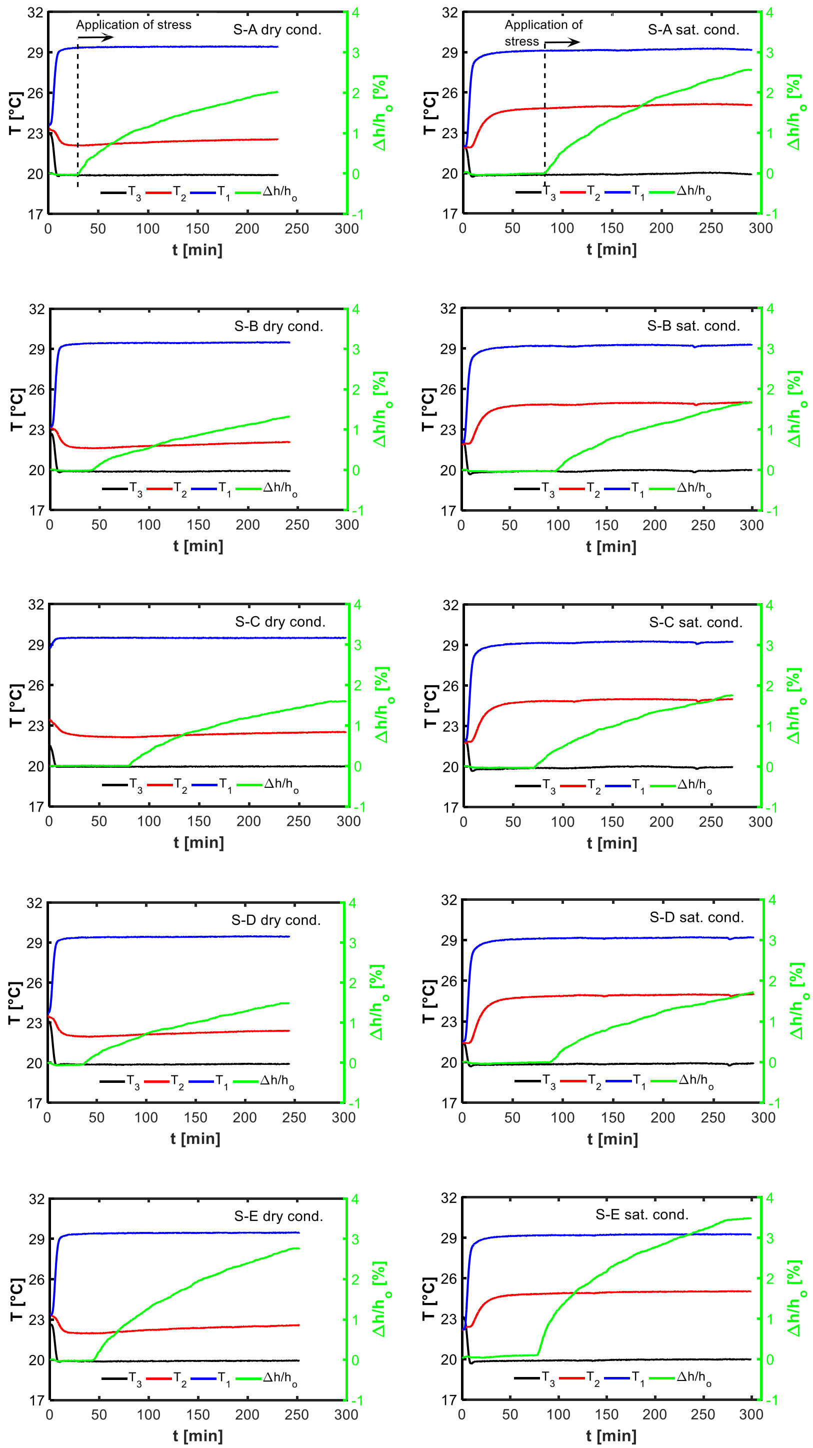

Figure 6. Temperature T and vertical strain $\Delta h/h_o$ plots for the steady state thermal conduction tests of the sandy soils as functions of time t

The consolidation times for the applied consolidation load (i.e. 400 and 200 minutes for the silty clay and sandy soils, respectively), which are inversely proportional to the selected rate of loading/shearing, are within the allowable limits provided by ASTM D 3080/D 3080M - 11 (2011) (i.e. 200 minutes for CL soils and 10 minutes for SP soils, USCS classification) ensuring that the effective stress is applied at a relatively slow rate, and the consolidation and shearing mechanisms of the specimens upon the application of the consolidation load do not produce excess pore-water pressure in the specimens for the tests performed under saturated conditions.

3 RESULTS AND DISCUSSION

In Figures 5 to 7, the results of the study of the variation of effective thermal conductivity λ of the studied soils with applied effective stress σ' are shown. In Figures 5 and 6, plots of the recorded temperatures of the three plates (i.e. top T_1, reference T_2 and bottom T_3) of the steady state device and the corresponding vertical strain $\Delta h/h_o$ of the specimens upon the application of effective stress are shown. The measured λ at each level of σ' for each soil type, obtained using the values of the measured temperatures of the three plates, is shown in Figure 7.

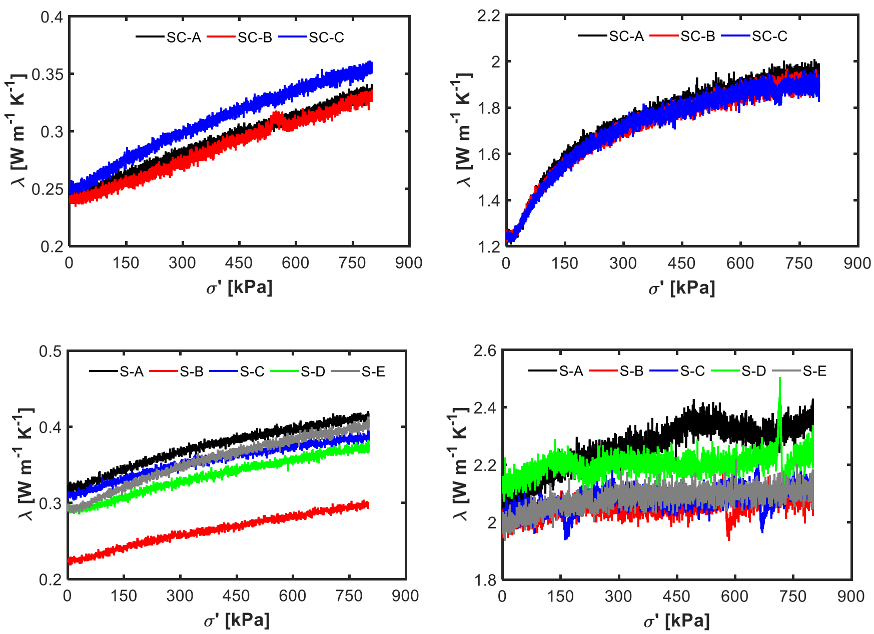

Figure 7. Effective thermal conductivity λ of the soils as a function of effective stress σ': dry condition (left) and saturated condition (right)

The sandy soils generally exhibit a higher thermal conductivity than the silty clay soils mainly due to their higher content of quartz fraction and higher density/lower porosity (Hailemariam etal., 2017). The measured temperature of the reference disc T_2 and hence the measured effective λ of the soils generally increase upon the application of stress, with a high rate of increase at the beginning (lower effective stress) and gradually slowing down at higher effective stress values following the load-deformation pattern of the loading tests.

Application of stress on a porous medium alters the inter-particle contact condition, by inducing changes in the internal structure or fabric of porous media (Choo et al., 2013), and generally causes an increase in the effective thermal conductivity of the medium mainly due to an increase in the inter-particle contact area and reduction of medium porosity. The reduction of medium porosity with the application of effective stress results in an increase of the medium's dry density, and the number of solid particles packed per unit volume increases improving the number and quality of contact points between the grains. As a result, the heat flow path, and consequently the effective thermal conductivity of the medium increases (Hailemariam etal., 2017).

In summary, application of effective stress on soils generally increases the effective thermal conductivity of soils following the load-deformation pattern, with a higher rate of increase in saturated as compared to dry conditions (mainly due to a higher rate of deformation or change of porosity of saturated soils as compared to dry soils upon the application of stress).

4 CONCLUSIONS

The variations of the effective thermal conductivities of three fine-grained and five coarse-grained soils with effective stress was analyzed under dry and saturated conditions with a steady state thermal conductivity and diffusivity meter. The measured effective thermal conductivities of the soils increased with the application of effective stress following the load-deformation pattern, with a higher magnitude of increase in saturated conditions as compared to dry conditions. The results indicate the significant influence stress has on the effective thermal conductivity of soils, which should be accounted for prior to their use as sensible heat storage systems.

5 ACKNOWLEDGEMENTS

The authors would like to acknowledge the financial support provided by the German Federal Ministry for Economic Affairs and Energy (BMWi) under Grant number 03ET6122A (Project ANGUS II).

6 REFERENCES

ASTM D 420 – D 5876. 2011. Soil and rock (I). ASTM International, West Conshohocken, PA, USA.

ASTM D 3080/D 3080M – 11. 2011. Standard test method for direct shear test of soils under consolidated drained conditions. ASTM International, West Conshohocken, PA, USA.

Birch, F., Clark, H. 1940. The thermal conductivity of rocks and its dependence upon temperature and composition, *American Journal of Science* **238**, 529–558.

Choo, J., Kim, Y.J., Lee, J.H., Yun, T.S., Lee, J., Kim, Y.S. 2013. Stress-induced evolution of anisotropic thermal conduc. of dry granular materials, *Acta Geotechnica* **8**, 91–106.

Hailemariam, H., Shrestha, D., Wuttke, F., Wagner, N. 2017. Thermal and dielectric behaviour of fine-grained soils, *Environmental Geotechnics* **4**, 79–93.

Hailemariam, H., Wuttke, F. 2018. Temperature dependency of the thermal conductivity of porous heat storage media, *Heat and Mass Transfer* **54**, 1031–1051.

Hart, G.K., Whiddon, W.I. 1984. Ground source heat pump planning workshop. Summary of Proceedings, Palo Alto: Electric Power Research Institute. EPRI Report RP 2033-12.

McGuinness, T., Hemmingway, P., Long, M. 2014. Design and development of a low-cost divided bar apparatus, *Geotechnical Testing Journal* **37**, 230–241.

Rosen, M.A., Hooper, F.C. 1989. A model for assessing the effects of berms on the heat loss from partially buried heat storage tanks. Proceedings, 9th International Heat Transfer Conference. Jerusalem, Israel.